European Journal of Phycology
2019, Volume 54, Issue 4, Pages 585-594
https://doi.org/10.1080/09670262.2019.1620342
https://archimer.ifremer.fr/doc/00505/61687/

Direct evidence for toxin production by *Pseudo-nitzschia plurisecta* (Bacillariophyceae) and extension of its distribution area

Caruana Amandine [1, *], Ayache Nour [1], Raimbault Virginie [1], Rétho Michael [2], Hervé Fabienne [1], Bilien Gwenael [3], Amzil Zouher [1], Chomérat Nicolas [3]

[1] IFREMER – Phycotoxin Laboratory, BP 21105, F – 44311 Nantes, France
[2] IFREMER/LER-MPL, BP 86, F – 56470 La Trinité sur Mer, France
[3] IFREMER/LER-BO, BP 40537, F – 29185 Concarneau, France

* Corresponding author : Amandine Caruana, email address : Amandine.Caruana@ifremer.fr

Abstract :

We confirm an amnesic shellfish poisoning risk associated with domoic acid production by the species *Pseudo-nitzschia plurisecta* and determine the toxin profile, which includes three domoic acid isomers. Although the species was reported once in European waters, along the Spanish Atlantic coast, here we describe and characterize P. plurisecta collected during the first occurrence in French Atlantic waters. Three strains (IFR-PPL-15.1, 15.2 and 15.3) were isolated from French coastal water samples in June 2015. These strains were identified and characterized by microscopic observation, molecular (ITS region sequencing and phylogenetic analysis) and metabolite (toxins and pigments) analyses. The cell shape is lanceolate and the valve contains a central interspace with uniseriate stria of oval-square poroids, each divided into 3–10 sectors. The ITS gene sequence is homologous to the original sequence available for the Spanish strain P. *plurisecta*. The pigment profile contains chl a, c3, c2, fucoxanthin, diatoxanthin, diadinoxanthin and traces of β,β-carotene. Results on morphology, phylogeny and pigments led to the identification of P. *plurisecta* and confirmed its first occurrence in French waters.

Keywords : Coastal monitoring, domoic acid, pigment composition, *Pseudo-nitzschia plurisecta*, taxonomic identification, toxic diatoms

46 Introduction

47 Several species of the marine diatom genus *Pseudo-nitzschia* are toxic due to
48 their ability to produce the phycotoxin Domoic Acid (DA) (Bates *et al.*, 1989; Bates *et*
49 *al.*, 2018; Caruana & Amzil, 2018). These diatoms bloom along coasts worldwide and
50 the DA they produce may accumulate in shellfish, causing amnesic shellfish poisoning
51 (ASP) in human consumers (Lelong *et al.*, 2012; Grattan *et al.*, 2016; Ajani *et al.*, 2018;
52 Wang *et al.*, 2018). Along French coasts, several toxigenic *Pseudo-nitzschia* species
53 have been reported since the first identification in 1998 of *Pseudo-nitzschia* species
54 associated with the detection of DA (Amzil *et al.*, 2001). These potentially toxic species
55 include *P. australis* Frenguelli, *P. multiseries* (Hasle) Hasle, *P. pseudodelicatissima*
56 (Hasle) Hasle, *P. pungens* (Grunow ex Cleve) G.R. Hasle, *P. fraudulenta* (Cleve) Hasle
57 and, less frequently, *P. calliantha* Lundholm, Moestrup & Hasle (Amzil *et al.*, 2001;
58 Nezan *et al.*, 2006; Quiroga, 2006). *Pseudo-nitzschia* populations generally develop
59 from March to September with maximum abundance in May-June. They proliferate
60 along the whole French coast including the Atlantic, English Channel and
61 Mediterranean seafronts. However, DA contamination events are mainly reported to
62 occur in the Atlantic areas of southern and western Brittany, where there are scallop
63 fisheries (Husson *et al.*, 2016). The risk of ASP is limited by screening and
64 identification of toxic *Pseudo-nitzschia* species. Regular screening for the neurotoxin
65 DA is made for shellfish flesh, and if DA contamination is detected, shellfish harvesting
66 areas are closed. This prevents contaminated seafood from being put on the market. DA
67 contamination causes huge economic losses to French scallop (*Pecten maximus*
68 Linnaeus) fisheries due to frequent and long-term accumulations of DA, which can last
69 from several months to a year (Blanco *et al.*, 2002; Belin & Amzil, 2010). Moreover,

70 DA may also contaminate other shellfish species such as those belonging to the genera
71 *Mytilus, Crassostrea, Donax, Glycymeris, Polititapes, Venerupis, Callista* and
72 *Cerastoderma* (Belin & Amzil, 2010). For the benefit of global public health, it is
73 necessary to survey, report and update the occurrence and diversity of *Pseudo-nitzschia*
74 species and their toxic potential worldwide.

75 The number of known *Pseudo-nitzschia* species has increased over the last
76 decade. In 2012, only 37 species of *Pseudo-nitzschia* were reported, of which 14 were
77 toxigenic (Lelong *et al*. 2012). Today, the genus *Pseudo-nitzschia* comprises 52 species
78 (Bates *et al.*, 2018; Guiry & Guiry, 2018) including 26 toxigenic species (Caruana &
79 Amzil, 2018; Lundholm, 2019). This rise in the number of toxic species described is a
80 result of increasing frequency and abundance of *Pseudo-nitzschia* blooms (Lundholm *et*
81 *al.*, 2010; Hinder *et al.*, 2012; Hernández-Fariñas *et al.*, 2014; Bazzoni *et al.*, 2015) and
82 technological advances. Indeed, there have been recent improvements in coastal
83 monitoring effort (Lelong *et al.*, 2012), and development of laboratory tools for species
84 identification (electron microscopy and molecular analyses) and high-sensitivity toxin
85 detection, all of which have become more accessible in terms of costs, facilities and
86 trained personnel. Available methods for toxin detection include the analytical
87 chemistry method LC-MS/MS, more affordable and widespread screening using the
88 biochemical method of ELISA assay that nevertheless requires confirmation by
89 chemical analysis, and the recent but more costly multitoxin Surface Plasmon
90 Resonance (SPR biosensor), (de la Iglesia *et al.*, 2013; McNamee *et al.*, 2016). As a
91 consequence of bloom frequency and scientific progress over recent years, novel species
92 have been identified and their toxicity demonstrated, e.g., *Pseudo-nitzschia simulans* Li,
93 Huang & Xu*, P. batesiana* Lim, Teng, Leaw & Lim, *P. kodamae* Teng, Lim, Leaw &

Lim and *P. fukuyoi* Lim, Teng, Leaw & Lim, (Lim *et al.*, 2013; Teng *et al.*, 2014; Dao *et al.*, 2015; Teng *et al.*, 2016; Li *et al.*, 2017). Furthermore, some species were shown to be toxic several years after their first taxonomic identification, when the opportunity arose to measure DA in monospecific blooms or isolated and cultivated algal cells. For instance, DA was detected in cells of *Pseudo-nitzschia cuspidata* (Hasle) Hasle, *P. brasiliana* Lundholm, Hasle & Fryxell, *P. cacianthа* Lundholm, Moestrup & Hasle, *P. subpacifica* (Hasle) Hasle and *P. obtusa* (Hasle) Hasle & Lundholm between 2009 and 2015 (Trainer *et al.*, 2009; Sahraoui *et al.*, 2011; Dao *et al.*, 2014; Fernandes *et al.*, 2014; Haroardottir *et al.*, 2015), although these species had all already been identified ten to fifty years earlier (Hasle, 1965; Lundholm *et al.*, 2002; Lundholm *et al.*, 2003). The toxic status of some species still needs to be confirmed, such as in the case of *P. hasleana* Lundholm, for which there is only one report of DA production (Sakka Hlaili *et al.*, 2016). In the case of *Pseudo-nitzschia plurisecta* Orive & Pérez-Aicua, the species was described by Orive *et al*. (2013) after being isolated in an estuary on the Spanish Atlantic coast. Prior to its description, an unnamed American species belonging to the same clade was isolated from the Gulf of Maine and shown to produce DA (Fernandes *et al.*, 2014). Based on the genetic affinities of this American strain with *P. plurisecta*, the diatom species was later listed among DA-producing species, but with an ambiguous reference due to the association of the toxin data with an anonymous strain (Zabaglo *et al.*, 2016). A more recent paper has since reported DA in two strains of *P. plurisecta* from Namibian waters (Gai *et al.*, 2018).

Here, we report further evidence of DA production by *P. plurisecta* as well as its first detection from the French Atlantic coast, supported by a detailed biological description and toxin profile.

Materials and Methods

Algal sampling, isolation and culture

A subsurface seawater sample (< 1 m) was collected (8 June 2015) in a Niskin bottle from the "Ouest Loscolo" station (GPS coordinates of 47.457596, -2.538268) by the French phytoplankton and phycotoxin monitoring network REPHY (Fig. 1). The water temperature was 15.7°C and salinity 33. *Pseudo-nitzschia* chains were isolated from fresh seawater samples under the microscope using an elongated Pasteur pipette and 4-well plates (Nunc, Thermo Fisher Scientific, Waltham, USA) filled with L1 medium for the rinsing steps of individual cells. Each isolated cell led to a clonal *Pseudo-nitzschia* strain that was then maintained in Erlenmeyer flasks for a few months by subculturing each week. Several strains, including three we named as IFR-PPL15.1, IFR-PPL15.2 and IFR-PPL15.3, were cultivated in batch cultures under 120 µmol photons m^{-2} s^{-1} light intensity. Cell density was enumerated by direct counting on a culture aliquot fixed with acidified Lugol's iodine and placed in a Nageotte counting chamber under a microscope. Two culture samples were used so that a mean could be calculated. Counts were made on 400 cells to limit deviation to 10% (Lund *et al.*, 1958).

Taxonomic identification

Taxonomic identification of *Pseudo-nitzschia* species was performed by coupling morphological and molecular identification results. Transmission electron microscopy (TEM, JEOL JEM-12-30 Tokyo, Japan) was carried out on the strain IFR-PPL-15.2 to study the detailed morphology of the frustules and confirm that the morphological characters agreed with the molecular identification (described below).

142 Frustules were cleaned with acid, rinsed in distilled water and then mounted on Formvar
143 grids according to the method described by Hasle (1978).
144
145 Molecular sequencing of rDNA ITS regions (ITS1, 5.8S, ITS2) was used to identify the
146 *Pseudo-nitzschia* strains maintained in laboratory cultures. PCRs were performed using
147 the oligonucleotide primers and protocols described in Nézan *et al*. (2014). The
148 sequences obtained were aligned together with 49 sequences of *Pseudo-nitzschia*
149 retrieved from GenBank using MAFFT v.7 software with the E-ins-I strategy (Katoh &
150 Standley, 2013). Unaligned parts of the matrix were removed using Gblocks 0.91b
151 (Castresana, 2000). The dataset comprising 52 sequences and 603 characters was
152 analysed by two methods of phylogenetic reconstruction: maximum likelihood (ML),
153 using PhyML v.3.0 (Guindon *et al.*, 2010) and Bayesian inference (BI) using MrBayes
154 v.3.2.6 (Ronquist & Huelsenbeck, 2003). jModeltest v.2.1.10 5 (Darriba *et al.*, 2012)
155 was first used to select the most suitable substitution model. The General Time-
156 Reversible model (GTR) with invariant sites (I) and gamma distribution with four
157 categories (G) was chosen, as indicated by Hierarchical Likelihood Ratio Tests
158 (hLRTs), Akaike Information Criterion 1 (AIC1), Akaike Information Criterion 2
159 (AIC2) and Bayesian Information Criterion (BIC) tests, implemented in jModeltest 2.
160 Bootstrap values of trees (indicating branch support) were obtained after 1000 iterations
161 in ML. For Bayesian inference, four Markov chains were run simultaneously for 2×10^6
162 generations with sampling every 100 generations. Of the 2×10^4 trees obtained, the first
163 2000 were discarded (burn-in) and a consensus tree was constructed from the remaining
164 trees. The posterior probabilities, corresponding to the frequency at which a node is

present in preserved trees, were calculated using a coupled Metropolis-Monte Carlo – Markov Chain (MCMC) approach.

Domoic acid analyses

Algal cell extracts of the three cultivated strains were analysed for intracellular toxins. First, cell pellets were obtained by centrifugation (3600 × g, 5 min) of 10 ml culture samples. The pellet was extracted in 1 ml methanol/water (50/50 v/v) and stored at -80°C until the subsequent steps were carried out. Defrosted cells were sonicated (20 min of intermittent 15 sec pulses at 5 sec intervals) with ice and ultracentrifuged (8000 × g, 0.2 µm, 15 min, Nanosep MF, Pall Corporation, East Hills, NY, USA) to obtain the supernatant. Samples were stored at -20°C until analyses. Ten µL of sample were injected into an Ultra Fast Liquid Chromatography (UFLC) system (Shimadzu, Marne-La-Vallée, France) coupled to 4000 QTrap tandem mass spectrometer (ABSciex, Les Ulis, France). The LC system was equipped with a Kinetex C18 precolumn (2.6 µm, 2 × 2.1 mm, Phenomenex, Le Pecq, France) and column (2.6 µm, 150 × 2.1 mm, Phenomenex). Flow rate was 0.2 ml min^{-1} and column temperature was 35°C. The mobile phase was composed of water as eluent A and 95% acetonitrile and 5% water as eluent B, both eluents containing 0.1% formic acid. The eluting gradient varied from 5 to 30% of eluent B in 14 min, then changed to 90% of B in 0.1 min and was maintained for 2.5 min before returning to initial conditions.

The LC-MS/MS system was used in MRM in positive mode. The following parameters were applied to the electrospray ionisation source: curtain gas 20 psi, temperature 550°C, gas1 50 psi, gas2 60 psi, ion spray voltage 5500 V. The following *m/z* transitions 312.1→266.1; 312.1→248.0; 312.1→220.0; 312.1→193.1 and

312.1→161.1 were used for identifying DA and some isomers. For detecting these fragments, the declustering potential was 60 V and the collision energies were 23, 25, 29, 27 and 33 eV for transitions 1 to 5, respectively. A calibration curve (0.5-250 ng ml^{-1}) based on a certified DA standard (CNRC, Halifax, Canada) prepared in methanol/water made it possible to perform quantification based on the most intense transition 312.1→266.1 (LD and LQ were respectively 0.1 and 0.25 ng ml^{-1}, respectively, corresponding to 1 and 2.5 pg DA on column). The commercial DA standard contains DA and traces of isodomoic acid-A, isodomoic acid-D and epi-DA among the nine existing isomers. Data were analysed with Analyst 1.5.1, ABSciex software and the cell toxin profile and toxin concentrations are given in fg per cell.

Pigment analyses

Pigment analyses were performed on the *P. plurisecta* strains. Fifty ml of culture were filtered on a 25 mm GF/F filter (Whatman, Maidstone, UK). The filter was snap-frozen in liquid N_2 and stored at -80°C until extraction. Pigments were extracted from cells by adding 1 ml of cold (4°C) 100% acetone. An internal standard (trans-β-apo-8'-carotenal, Sigma-Aldrich, Saint-Quentin-Fallavier, France) was also added at this stage to allow final corrections according to the extraction yield. Cell lyses were stimulated using an ultrasonic bath filled with ice (10 min, twice) and the sample was stored for 6 to 24 hours at -20°C in darkness. Debris was removed by filtration of the supernatant on a PTFE 0.2-µm membrane. Sample aliquots of 30 µl were supplemented with 45 µl of ultrapure water and analysed by Liquid Chromatography with Diode Array Detection (LC-DAD). The 1200 LC-DAD (Agilent Technologies, Massy, France) apparatus was

212 set up with a precolumn (XSelect HSS T3, 3.5 µm, 20 × 3 mm, Waters) and a C_{18}
213 column (XSelect HSS T3, 3.5 µm, 150 × 3 mm, Waters).

214 The LC-DAD method was adapted from Zapata *et al*. (2012) and used the same
215 eluents as that previous study, but gradients were modified to improve peak separation.
216 Hence, four eluents were used: A: methanol, B: acetonitrile, C: pyridine (25 mM, pH 5)
217 and D: acetone (Sigma-Aldrich). The initial mobile phase was composed of
218 A:B:C:D=45:38:17:0 (v/v/v/v) from t_0 to t_3, with time (t) expressed in minutes. The
219 gradient of elution then evolved to 35:50:15:0 between t_3 and t_{20} and to 20:60:0:20
220 between t_{20} and t_{25}. It then evolved to 0:60:0:40 between t_{25} and t_{35} and remained at
221 these proportions until t_{43} before finally returning to the initial mobile phase at t_{45}. Flow
222 rate was 0.6 ml min^{-1} and column temperature was 30°C. Data were collected with the
223 OpenLab CDS Chemstation C.01.07 program.

224 Pigments were identified by their retention time and comparison of the
225 absorbance spectra between 350 and 700 nm with those obtained with commercial
226 standards. Pigment quantification was done at two wavelengths according to the
227 maximum absorbance wavelengths of the pigments: 436 nm for chl *a* and 450 nm for
228 the others. Commercial standards (DHI Water Environment Health, Hørsholm,
229 Denmark) for each pigment were used with calibration curves, for identification and
230 quantification of the pigments in the algal cell extracts.

231 Algal cells from each strain in triplicate batch cultures were sampled several
232 times during culture growth (at days 3, 7 and 10 for strain IFR-PPL-15.1, at days 2, 5, 6,
233 9, 10 for strain IFR-PPL-15.2 and at days 6 and 9 for strain IFR-PPL-15.3). Range data
234 and means are given to cover potential growth variation. Data are displayed in several

235 units: fg per cell, mol per mol of chl *a*, µg per L of culture and as a percentage of total
236 pigments. Sample extractions and analyses were performed under weak light conditions.
237
238 Results
239 *Strain identification*
240 The *Pseudo-nitzschia* strains IFR-PPL-15.1, 15.2 and 15.3 isolated from the
241 "Ouest Loscolo" station on the French Atlantic coast (Fig. 1) in 2015, were identified as
242 *Pseudo-nitzschia plurisecta* according to their morphological characters (Figs. 2-8) and
243 the molecular analyses (Fig. 9). Based on the ITS region, the three strains were
244 genetically identical. Morphologically, frustules of the culture IFR-PPL-15.2 were
245 lanceolate, 23.3-29.7 µm long (mean 26.0 ± 1.4 µm, n = 30) and 1.9-2.5 µm wide (mean
246 2.2 ± 0.2 µm, n = 30). A central interspace (Fig. 6) was present on the valves. The
247 number of striae in 10 µm was 37-41 while the number of fibulae in 10 µm was 22-25.
248 Each stria was uniseriate and contained one row of oval-square poroids, with 5 to 7
249 poroids in 1 µm. Each poroid was split into 3 to 10 sectors, with a few possessing a
250 central sector (Fig. 7), as previously shown for *P. plurisecta* (Orive *et al.*, 2013). As in
251 *P. australis* (Amato *et al.*, 2005), when cultivated in artificial medium, *P. plurisecta*
252 rapidly showed cell deformation as illustrated by several humps on each side of the
253 frustule (Fig. 2).
254 The phylogenetic analysis revealed that the sequences of strains IFR-PPL-15.1,
255 15.2 and 15.3 were identical to sequence KC409089 of strain Ner-F1, isolated from
256 Bilbao outer estuary and considered as the type strain for *P. plurisecta* (Orive *et al.*,
257 2013). Notably, a sequence (IFR997) previously acquired from a single-chain isolated
258 in the Bay of Concarneau in 2009 (Fig. 1; GPS coordinates 47.833406, -3.949922),

clustered with and corresponds to *P. plurisecta* (Fig. 9). Likewise, a 2016 isolate (IFR-PPL-16) from the REPHY "Men er Roué" Atlantic sampling station (GPS coordinates of 47.534765, -3.093748) is now genetically identified as *P. plurisecta*.

Strain toxicity

For the three *P. plurisecta* strains IFR-PPL-15.1, 15.2 and 15.3, toxin analyses of cell extracts revealed a similar DA chromatographic profiles compared with the standard profile for DA. The DA peak appeared at a retention time of 8.1 min with five transition ions: 312.1 → 266.1, 248.0, 220.0, 193.1 and 161.1. For clarity, only the most and least intense transitions (312.1 →266.1 and 161.1) are shown on Figures 10-13. Several peaks of DA isomers were observed. Based on the comparison of their retention time with those of the DA standard, these isomers were identified as possibly being isodomoic acid-A and epi-DA in the three *P. plurisecta* strains and isodomoic acid-D in the strain IFR-PPL-15.3. The three strains contain DA at 3.1, 3.9 and 58.3 fg $cell^{-1}$, respectively (Table 1).

Pigment analyses

Pigment analyses (Table 2) confirmed the presence of chlorophylls *a*, c_3 and c_2, the carotenoids fucoxanthin, diatoxanthin, diadinoxanthin and traces of β,β-carotene in the three strains of *P. plurisecta*. Although the pigment ratio could vary during growth in batch culture, chl *a* and fucoxanthin were the major pigments, each accounting for between a third and half of the total pigments. Apart from fucoxanthin, chl c_3 was the other main accessory pigment (reaching a maximum of 10 %). Chl c_2, diadinoxanthin

283 and diatoxanthin were minor pigments (< 7% for each). β,β-carotene was present at
284 trace level (< 2%). The ratios of major accessory pigments to chl *a* are in the ranges of
285 0.834-1.439, 0.164-0.209 and 0.194-0.325 for fucoxanthin, chl c_2 and chl c_3,
286 respectively.
287
288 Discussion
289 The morpho-molecular analyses performed in the present study unambiguously
290 confirm that strains IFR-PPL-15.1, 15.2 and 15.3 correspond to *Pseudo-nitzschia*
291 *plurisecta*. However, their morphology was analysed on aged cultures and the cell
292 dimensions (mean length 26.0 µm) were not in the same range (56-60 µm) as those
293 given in the original description of the Spanish strain (Orive *et al*. 2013). Nevertheless,
294 the detailed characters of striae, fibulae and poroid arrangement were the same as given
295 by these previous authors, which allows us to confirm the species identification. Based
296 on molecular data, our study demonstrates that this species was already present in June
297 2009 in the northern part of the Bay of Biscay (France), before its description by Orive
298 *et al*. (2013), and was observed again in 2016, confirming its recurrence in the
299 phytoplankton community.
300 In terms of toxin production, *P. plurisecta* is confirmed to produce DA and is
301 rightfully categorized as a toxic species. *P. plurisecta* is thus an additional toxigenic
302 species that may be present in *Pseudo-nitzschia* populations in French coastal waters,
303 contributing to ASP risk. The DA content of *P. plurisecta* varies among strains in
304 laboratory cultures, potentially due to diversity of cell sizes, growth phases or
305 phenotypes. The French strains show a 17-fold variation of DA concentration (3-59 fg
306 $cell^{-1}$), while American and Namibian strains contain a 6-fold higher DA concentration

(19-385 fg cell^{-1}; Fernandes *et al*. 2014; Gai *et al*. 2018). The lower DA content of French *P. plurisecta* strains may result from the smaller cell size (23-30 µm length in comparison with 30 - 54 µm for the American strain). Indeed, DA content generally decreases with culture ageing and smaller cell size in *Pseudo-nitzschia* (Mafra *et al.*, 2009). *P. plurisecta* appears to produce a much lower concentration of DA than the most toxigenic species *P. australis* or *P. multiseries* that also proliferate along the French coasts and other parts of the world, producing up to 78 and 67 pg DA cell^{-1} respectively (Lelong *et al.*, 2012; Trainer *et al.*, 2012). However, *P. plurisecta* produces an equivalent or higher DA concentration than most other toxigenic *Pseudo-nitzschia* species (reviewed in Trainer *et al*. 2012 and Lelong *et al*. 2012).

The toxin profile of *P. plurisecta* is composed of DA and three DA isomers whose, identities, based on an incomplete panel of standards, remain uncertain and would require further RMN analyses. So far, isodomoic acid-A, -B and -C have been identified in some *Pseudo-nitzschia* spp. and traces of isodomoic acid-D, -E and epi-DA have been identified in *Nitzschia navis-varingica* (Holland *et al.*, 2005; Hansen *et al.*, 2011; Romero *et al.*, 2011). According to published chromatographic data (Romero *et al.*, 2011), DA isomers in *P. plurisecta* cells are most likely to be isodomoic acid-D and -A. Here, it is also proposed that epi-DA is present in *P. plurisecta* cells, and a possible contribution of isodomoic acid-B to the epi-DA peak cannot be excluded. *P. plurisecta* may represent a significant source of DA contamination for countries with coasts along the Atlantic Ocean. Further ecophysiological studies on this species are needed to precisely determine its DA producing capacity in relation to growth phases, environmental conditions and strain variability and to confirm the DA isomer identities.

330 The pigment composition of *P. plurisecta* observed here is similar to that
331 described by Orive *et al*. (2013). *P. plurisecta* appears to have the most common
332 pigment type of *Pseudo-nitzschia* species: type 3 as described by Zapata *et al*. (2011),
333 like the toxic *Pseudo-nitzschia* species: *P. calliantha*, *P. cuspidata*, *P. delicatissima*, *P.*
334 *galaxiae* and *P. pseudodelicatissima*, while some other toxic *Pseudo-nitzschia* species
335 belong to pigment types 1 or 2. The pigment composition of *P. plurisecta* shows some
336 differences from other *Pseudo-nitzschia* species. Although chl *a* and fucoxanthin are
337 found to be the major pigments here as in other *Pseudo-nitzschia* spp. (Quijano-
338 Scheggia *et al.*, 2008; Zapata *et al.*, 2011), chl c_1, chl c_2-like, MgDVP, cis-fucoxanthin
339 and chlorophyllide were not detected in our *P. plurisecta* cultures or in the previously
340 reported occurrence (Orive *et al.*, 2013). Chl c_3 is the second most important accessory
341 pigment, as in *P. delicatissima* (Quijano-Scheggia *et al.*, 2008), while chl c_2 is generally
342 found as the dominant chl *c*-type pigment in other *Pseudo-nitzschia* species. The most
343 toxic species, *P. australis* and *P. multiseries*, contain chl c_2 but not chl c_3. Zapata *et al*.
344 (2011) observed that the ratios of accessory pigments to chl *a* (fuco: chl *a* or chl c_2 : chl
345 *a*) are conserved among 49 *Pseudo-nitzschia* strains belonging to 17 species (0.448-
346 1.130, 0.150-0.424, respectively) while the chl c_3 to chl *a* ratio is naturally more
347 variable (0-0.313). In *P. plurisecta* cells, apart from the slightly higher ratio of fuco : chl
348 *a*, the ratios chl c_2 : chl *a* and chl c_3 : chl *a* are within similar ranges to those described
349 by Zapata *et al*. (2011).
350 *Pseudo-nitzschia plurisecta* is distributed on both sides of the North Atlantic
351 Ocean, including along the European coast (Orive *et al.*, 2013), Gulf of Maine
352 (Fernandes *et al.*, 2014); it is also found in Namibian waters in the South Atlantic Ocean
353 (Gai *et al.*, 2018). This distribution appears limited due to the recent description of this

354 species and might expand in the future. Along the European coast, the occurrence of this
355 species seems to be favoured by estuarine influences as observed in the Bilbao Estuary
356 in Spain and the Vilaine Estuary in France. Along the French coast, the proliferation of
357 *Pseudo-nitzschia* populations appears to be facilitated by nutrient-rich waters in
358 confined or semi-enclosed bays enriched by river input and benthic sediment mixing
359 (Husson *et al.*, 2016). Moreover, the increasing abundance of *Pseudo-nitzschia*
360 populations along the French coast, between 1992 and 2011, reported by Hernández-
361 Fariñas *et al*. (2015), may lead to the observation of new or rare *Pseudo-nitzschia*
362 species. Consequently, eutrophic waters potentially represent a nursery for new *Pseudo-*
363 *nitzschia* species, suggesting that eutrophication may not only influence the abundance
364 but also the richness in toxic species.

365 Regarding shellfish farming management, further investigations are required to
366 understand what favours the occurrence of toxic *Pseudo-nitzschia* species compared
367 with non-toxic ones and their possible relation with other phytoplankton species. For
368 instance, more data on species assemblages and succession would be helpful to
369 investigate whether there exists a link between changes in species assemblages and the
370 observed rise in toxic species occurrence. In the present study, *P. plurisecta* was
371 isolated in association with non-toxic strains of *P. fraudulenta* and *P. pungens* (SEM
372 photographs in supplementary files). In Namibian waters, *P. plurisecta* was found with
373 *P. bucculenta* or *P. pungens* and *P. australis* (Gai *et al.*, 2018). In a study along the
374 English Channel, Klein *et al*. (2010) observed the succession of several *Pseudo-*
375 *nitzschia* species in relation, although not exclusively, to peak concentrations of NO_3 or
376 NH_4. Interestingly, the authors found that *P. australis* occurred under high NH_4 and low
377 NO_3 concentrations, while *P. delicatissima*, *P. fraudulenta* and *P. multistriata* preferred

high NO_3 concentrations. However, other environmental factors may also influence *Pseudo-nitzschia* population dynamics, such as irradiance and temperature conditions triggering the bloom initiation and, over a decadal timescale, changes in salinity, temperature and the Atlantic multidecadal oscillation index that may become favourable to the development of *Pseudo-nitzschia* populations (Hernández-Fariñas *et al.*, 2014; Husson *et al.*, 2016).

Our study confirms DA production by *Pseudo-nitzschia plurisecta* and provides a detailed description of the species. *P. plurisecta* cells were shown to contain DA and three isomers that are potentially isodomoic acid-A, -D and epi-DA. Because *P. plurisecta* can pose a severe risk of Amnesic Shellfish Poisoning to humans and is known to be present in Atlantic coastal and estuarian areas, it is important to list *P. plurisecta* as a toxic *Pseudo-nitzschia* species (Lundholm, 2019). The increase in *Pseudo-nitzschia* populations means that further ecological and ecophysiological investigations should be encouraged to enhance our knowledge of the ecological niche and DA production capacity of *P. plurisecta*.

Acknowledgements

This work was supported by IFREMER through the internal funding of the ECOPSEUDO project on *Pseudo-nitzschia*. We are also grateful to Cédric Gaillard of the BIBS Platform at INRA Nantes for allowing us to produce the TEM photographs.

400 References

401 Ajani, P.A., Verma, A., Lassudrie, M., Doblin, M.A., & Murray, S.A. (2018). A new
402 diatom species *P. hallegraeffii* sp. nov. belonging to the toxic genus *Pseudo-nitzschia*
403 (Bacillariophyceae) from the East Australian Current. *Plos One* **13**: 20.
404 Amato, A., Orsini, L., D'alelio, D., & Montresor, M. (2005). Life cycle, size reduction
405 patterns, and ultrastructure of the pennate planktonic diatom *Pseudo-nitzschia*
406 *delicatissima* (Bacillariophyceae). *Journal of Phycology* **41**: 542-556.
407 Amzil, Z., Fresnel, J., Le Gal, D., & Billard, C. (2001). Domoic acid accumulation in
408 French shellfish in relation to toxic species of *Pseudo-nitzschia multiseries* and *P.*
409 *pseudodelicatissima*. *Toxicon* **39**: 1245-1251.
410 Bates, S.S., Bird, C.J., Defreitas, A.S.W., Foxall, R., Gilgan, M., Hanic, L.A., Johnson,
411 G.R., Mcculloch, A.W., Odense, P., Pocklington, R., Quilliam, M.A., Sim, P.G., Smith,
412 J.C., Rao, D.V.S., Todd, E.C.D., Walter, J.A., & Wright, J.L.C. (1989). Pennate diatom
413 *Nitzschia-pungens* as the primary source of domoic acid, a toxin in shellfish from
414 eastern Prince Edward Island, Canada. *Canadian Journal of Fisheries and Aquatic*
415 *Sciences* **46**: 1203-1215.
416 Bates, S.S., Hubbard, K.A., Lundholm, N., Montresor, M., & Leaw, C.P. (2018).
417 *Pseudo-nitzschia*, *Nitzschia*, and domoic acid: New research since 2011. *Harmful Algae*
418 **79**: 3-43.
419 Bazzoni, A.M., Caddeo, T., Pulina, S., Padedda, B.M., Satta, C.T., Sechi, N., & Luglie,
420 A. (2015). Spatial distribution and multiannual trends of potentially toxic microalgae in
421 shellfish farms along the Sardinian coast (NW Mediterranean Sea). *Environmental*
422 *Monitoring and Assessment* **187**.

423 Belin, C. & Amzil, Z. (2010). Phycotoxin monitoring in France : risk-based strategy and
424 main results (2006-2008). In *Proceedings of the 7th International Conference on*
425 *Molluscan Shellfish Safety* (Lassus, P., editor), 149-156. Ifremer, Nantes.
426 Blanco, J., Acosta, C.P., De La Puente, M.B., & Salgado, C. (2002). Depuration and
427 anatomical distribution of the amnesic shellfish poisoning (ASP) toxin domoic acid in
428 the king scallop *Pecten maximus*. *Aquatic Toxicology* **60**: 111-121.
429 Caruana, A.M.N. & Amzil, Z. (2018). Chapter 13 - Microalgae and Toxins. In
430 *Microalgae in Health and Disease Prevention* (Levine, I.A. & Fleurence, J., editors),
431 263-305. Academic Press, London.
432 Castresana, J. (2000). Selection of conserved blocks from multiple alignments for their
433 use in phylogenetic analysis. *Molecular Biology and Evolution* **17**: 540-552.
434 Dao, H.V., Lim, P.T., Ky, P.X., Takata, Y., Teng, S.T., Omura, T., Fukuyo, Y., &
435 Kodama, M. (2014). Diatom *Pseudo-nitzschia* cf. *caciantha* (Bacillariophyceae), the
436 most likely source of domoic acid contamination in the thorny oyster *Spondylus*
437 *versicolor* Schreibers 1793 in Nha Phu Bay, Khanh Hoa Province, Vietnam. . *Asian*
438 *Fish. Sci.* **27**: 16–29.
439 Dao, H.V., Phan, V.B., Teng, S.T., Uchida, H., Leaw, C.P., Lim, P.T., Suzuki, T., &
440 Pham, K.X. (2015). *Pseudo-nitzschia fukuyoi* (Bacillariophyceae), a domoic acid-
441 producing species from Nha Phu Bay, Khanh Hoa Province, Vietnam. *Fisheries Science*
442 **81**: 533-539.
443 Darriba, D., Taboada, G.L., Doallo, R., & Posada, D. (2012). jModelTest 2: more
444 models, new heuristics and parallel computing. *Nature Methods* **9**: 772-772.
445 De La Iglesia, P., Fernandez-Tejedor, M., Trobajo, R., & Diogene, J. (2013). An
446 analytical perspective on detection, screening, and confirmation in phycology, with

447 particular reference to toxins and toxin-producing species. *Journal of Phycology* **49**:
448 1056-1060.
449 Fernandes, L.F., Hubbard, K.A., Richlen, M.L., Smith, J., Bates, S.S., Ehrman, J.,
450 Leger, C., Mafra, L.L., Kulis, D., Quilliam, M., Libera, K., Mccauley, L., & Anderson,
451 D.M. (2014). Diversity and toxicity of the diatom *Pseudo-nitzschia* Peragallo in the
452 Gulf of Maine, Northwestern Atlantic Ocean. *Deep-Sea Research Part Ii-Topical*
453 *Studies in Oceanography* **103**: 139-162.
454 Gai, F.F., Hedemand, C.K., Louw, D.C., Grobler, K., Krock, B., Moestrup, O., &
455 Lundholm, N. (2018). Morphological, molecular and toxigenic characteristics of
456 Namibian *Pseudo-nitzschia* species - including *Pseudo-nitzschia bucculenta* sp nov.
457 *Harmful Algae* **76**: 80-95.
458 Grattan, L.M., Holobaugh, S., & Morris, J.G. (2016). Harmful algal blooms and public
459 health. *Harmful Algae* **57**: 2-8.
460 Guindon, S., Dufayard, J.F., Lefort, V., Anisimova, M., Hordijk, W., & Gascuel, O.
461 (2010). New algorithms and methods to estimate Maximum-Likelihood phylogenies:
462 assessing the performance of PhyML 3.0. *Systematic Biology* **59**: 307-321.
463 Guiry, M.D. & Guiry, G.M. (2018). AlgaeBase. World-wide electronic publication,
464 National University of Ireland, Galway. http://www.algaebase.org; searched on 24
465 September 2018.
466 Hansen, L.R., Soylu, S.I., Kotaki, Y., Moestrup, O., & Lundholm, N. (2011). Toxin
467 production and temperature-induced morphological variation of the diatom *Pseudo-*
468 *nitzschia seriata* from the Arctic. *Harmful Algae* **10**: 689-696.
469 Haroardottir, S., Pancic, M., Tammilehto, A., Krock, B., Moller, E.F., Nielsen, T.G., &
470 Lundholm, N. (2015). Dangerous relations in the Arctic marine food web: Interactions

471 between toxin producing *Pseudo-nitzschia* diatoms and *Calanus* copepodites. *Marine*
472 *Drugs* **13**: 3809-3835.
473 Hasle, G.R. (1965). *Nitzschia* and *Fragilariopsis* species studied in the light and
474 electron microscopes. II. The group *Pseudo-nitzschia.* Skrifter utgitt av Det Norske
475 Videnskaps-Akademii Oslo . I. Matematisk-Naturvidenskapelig Klasse. Series 18:1-45.
476 Hasle, G.R. (1978). Some specific preparations: diatoms. In *Phytoplankton manual.*
477 (Sournia, A., editor), 136-142. UNESCO, Paris.
478 Hernández-Fariñas, T. (2015). Analyse et modélisation des évolutions à long terme de
479 la biodiversité phytoplanctonique dans les zones côtières sous l'effet des pressions
480 environnementales et anthropiques. Ph.D. dissertation. University of Nantes, France,
481 352 pp.
482 Hernández-Fariñas, T., Soudant, D., Barille, L., Belin, C., Lefebvre, A., & Bacher, C.
483 (2014). Temporal changes in the phytoplankton community along the French coast of
484 the eastern English Channel and the southern Bight of the North Sea. *Ices Journal of*
485 *Marine Science* **71**: 821-833.
486 Hinder, S.L., Hays, G.C., Edwards, M., Roberts, E.C., Walne, A.W., & Gravenor, M.B.
487 (2012). Changes in marine dinoflagellate and diatom abundance under climate change.
488 *Nature Climate Change* **2**: 271-275.
489 Holland, P.T., Selwood, A.I., Mountfort, D.O., Wilkins, A.L., Mcnabb, P., Rhodes,
490 L.L., Doucette, G.J., Mikulski, C.M., & King, K.L. (2005). Isodomoic acid C, an
491 unusual amnesic shellfish poisoning toxin from *Pseudo-nitzschia australis*. *Chemical*
492 *Research in Toxicology* **18**: 814-816.
493 Husson, B., Hernandez-Farinas, T., Le Gendre, R., Schapira, M., & Chapelle, A. (2016).
494 Two decades of *Pseudo-nitzschia* spp. blooms and king scallop (*Pecten maximus*)

495 contamination by domoic acid along the French Atlantic and English Channel coasts:
496 Seasonal dynamics, spatial heterogeneity and interannual variability. *Harmful Algae* **51**:
497 26-39.
498 Katoh, K. & Standley, D.M. (2013). MAFFT multiple sequence alignment software
499 version 7: improvements in performance and usability. *Molecular Biology and*
500 *Evolution* **30**: 772-780.
501 Klein, C., Claquin, P., Bouchart, V., Le Roy, B., & Veron, B. (2010). Dynamics of
502 *Pseudo-nitzschia* spp. and domoic acid production in a macrotidal ecosystem of the
503 Eastern English Channel (Normandy, France). *Harmful Algae* **9**: 218-226.
504 Lelong, A., Hegaret, H., Soudant, P., & Bates, S.S. (2012). *Pseudo-nitzschia*
505 (Bacillariophyceae) species, domoic acid and amnesic shellfish poisoning: revisiting
506 previous paradigms. *Phycologia* **51**: 168-216.
507 Li, Y., Huang, C.X., Xu, G.S., Lundholm, N., Teng, S.T., Wu, H., & Tan, Z. (2017).
508 *Pseudo-nitzschia simulans* sp. nov. (Bacillariophyceae), the first domoic acid producer
509 from Chinese waters. *Harmful Algae* **67**: 119-130.
510 Lim, H.C., Teng, S.T., Leaw, C.P., & Lim, P.T. (2013). Three novel species in the
511 *Pseudo-nitzschia pseudodelicatissima* complex: *P. batesiana* sp nov., *P lundholmiae* sp
512 nov., and *P. fukuyoi* sp nov. (Bacillariophyceae) from the strait of Malacca, Malaysia.
513 *Journal of Phycology* **49**: 902-916.
514 Lund, J.W.G., Kipling, C., & Lecren, E.D. (1958). The inverted microscope method of
515 estimating algal numbers and the statistical basis of estimations of counting.
516 *Hydrobiologia* **11**: 143–170.

517 Lundholm, N. (2019). (Ed) Bacillariophyceae, in IOC-UNESCO Taxonomic Reference
518 List of Harmful Micro Algae. Available online at http://www.marinespecies.org/hab.
519 Accessed on 2019-03-20.
520 Lundholm, N., Clarke, A., & Ellegaard, M. (2010). A 100-year record of changing
521 *Pseudo-nitzschia* species in a sill-fjord in Denmark related to nitrogen loading and
522 temperature. *Harmful Algae* **9**: 449-457.
523 Lundholm, N., Hasle, G.R., Fryxell, G.A., & Hargraves, P.E. (2002). Morphology,
524 phylogeny and taxonomy of species within the *Pseudo-nitzschia americana* complex
525 (Bacillariophyceae) with descriptions of two new species, *Pseudo-nitzschia brasiliana*
526 and *Pseudo-nitzschia linea*. *Phycologia* **41**: 480-497.
527 Lundholm, N., Moestrup, O., Hasle, G.R., & Hoef-Emden, K. (2003). A study of the
528 *Pseudo-nitzschia pseudodelicatissima/cuspidata* complex (Bacillariophyceae): What is
529 *P. pseudodelicatissima*? *Journal of Phycology* **39**: 797-813.
530 Mafra, L.L., Bricelj, V.M., Ouellette, C., Leger, C., & Bates, S.S. (2009). Mechanisms
531 contributing to low domoic acid uptake by oysters feeding on *Pseudo-nitzschia* cells. I.
532 Filtration and pseudofeces production. *Aquatic Biology* **6**: 201-212.
533 Mcnamee, S.E., Medlin, L.K., Kegel, J., Mccoy, G.R., Raine, R., Barra, L., Ruggiero,
534 M.V., Kooistra, W., Montresor, M., Hagstrom, J., Blanco, E.P., Graneli, E., Rodriguez,
535 F., Escalera, L., Reguera, B., Dittami, S., Edvardsen, B., Taylor, J., Lewis, J.M., Pazos,
536 Y., Elliott, C.T., & Campbell, K. (2016). Distribution, occurrence and biotoxin
537 composition of the main shellfish toxin producing microalgae within European waters:
538 A comparison of methods of analysis. *Harmful Algae* **55**: 112-120.

539 Nézan, E., Antoine, E., Fiant, L., Amzil, Z., & Billard, C. (2006). Identification of
540 *Pseudonitzschia australis* and *P. multiseries* in the Bay of Seine. Was there a relation to
541 presence of domoic acid in king scallops in autumn 2004? *Harmful Algae News* **31**: 1-3.
542 Nézan, E., Siano, R., Boulben, S., Six, C., Bilien, G., Chèze, K., Duval, A., Le Panse,
543 S., Quéré, J., & Chomérat, N. (2014). Genetic diversity of the harmful family
544 Kareniaceae (Gymnodiniales, Dinophyceae) in France, with the description of
545 *Karlodinium gentienii* sp nov.: A new potentially toxic dinoflagellate. *Harmful Algae*
546 **40**: 75-91.
547 Orive, E., Perez-Aicua, L., David, H., Garcia-Etxebarria, K., Laza-Martinez, A.,
548 Seoane, S., & Miguel, I. (2013). The genus *Pseudo-nitzschia* (Bacillariophyceae) in a
549 temperate estuary with descritpion of two new species: *Pseudo-nitzschia plurisecta* sp
550 nov and *Pseudo-nitzschia abrensis* sp nov. *Journal of Phycology* **49**: 1192-1206.
551 Quijano-Scheggia, S., Garces, E., Sampedro, N., Van Lenning, K., Flo, E., Andree, K.,
552 Fortuno, J.M., & Camp, J. (2008). Identification and characterisation of the dominant
553 *Pseudo-nitzschia* species (Bacillariophyceae) along the NE Spanish coast (Catalonia,
554 NW Mediterranean). *Scientia Marina* **72**: 343-359.
555 Quiroga, I. (2006). *Pseudo-nitzschia* blooms in the Bay of Banyuls-sur-Mer,
556 northwestern Mediterranean Sea. *Diatom Research* **21**: 91-104.
557 Romero, M.L.J., Kotaki, Y., Lundholm, N., Thoha, H., Ogawa, H., Relox, J.R., Terada,
558 R., Takeda, S., Takata, Y., Haraguchi, K., Endo, T., Lim, P.-T., Kodama, M., &
559 Fukuyo, Y. (2011). Unique amnesic shellfish toxin composition found in the South East
560 Asian diatom *Nitzschia navis-varingica*. *Harmful Algae* **10**: 456-462.
561 Ronquist, F. & Huelsenbeck, J.P. (2003). MrBayes 3: Bayesian phylogenetic inference
562 under mixed models. *Bioinformatics* **19**: 1572-1574.

563 Sahraoui, I., Bates, S.S., Bouchouicha, D., Mabrouk, H.H., & Hlaili, A.S. (2011).
564 Toxicity of *Pseudo-nitzschia* populations from Bizerte Lagoon, Tunisia, southwest
565 Mediterranean, and first report of domoic acid production by *P. brasiliana*. *Diatom*
566 *Research* **26**: 293-303.
567 Sakka Hlaili, A., Sahraoui Khalifa, I., Bouchouicha-Smida, D., Sondes Melliti Garali,
568 K., J., , Chalghaf, M., Bates, S.S., Lundholm, N., Kooistra, W., De La Iglesia, P., &
569 Diogène, J. (2016). Toxic and potentially toxic diatom blooms in Tunisian (SW
570 Mediterranean) waters: Review of ten years of investigations In *Advances in*
571 *Environmental Research* (48) (Daniels, J.A., editor), 51-69. Nova Science Publishers,
572 Inc.
573 Teng, S.T., Lim, H.C., Lim, P.T., Dao, V.H., Bates, S.S., & Leaw, C.P. (2014). *Pseudo-*
574 *nitzschia kodamae* sp. nov. (Bacillariophyceae), a toxigenic species from the Strait of
575 Malacca, Malaysia. *Harmful Algae* **34**: 17-28.
576 Teng, S.T., Tan, S.N., Lim, H.C., Dao, V.H., Bates, S.S., & Leaw, C.P. (2016). High
577 diversity of *Pseudo-nitzschia* along the northern coast of Sarawak (Malaysian Borneo),
578 with descriptions of *P. bipertita* sp. nov. and *P. limii* sp. nov. (Bacillariophyceae).
579 *Journal of Phycology* **52**: 973-989.
580 Trainer, V.L., Bates, S.S., Lundholm, N., Thessen, A.E., Cochlan, W.P., Adams, N.G.,
581 & Trick, C.G. (2012). *Pseudo-nitzschia* physiological ecology, phylogeny, toxicity,
582 monitoring and impacts on ecosystem health. *Harmful Algae* **14**: 271-300.
583 Trainer, V.L., Wells, M.L., Cochlan, W.P., Trick, C.G., Bill, B.D., Baugh, K.A., Beall,
584 B.F., Herndon, J., & Lundholm, N. (2009). An ecological study of a massive bloom of
585 toxigenic *Pseudo-nitzschia cuspidata* off the Washington State coast. *Limnology and*
586 *Oceanography* **54**: 1461-1474.

587 Wang, Y., Xiang, P., Kang, J.H., Ye, Y.Y., Lin, G.M., Yang, Q.L., & Lin, M. (2018).
588 Microphytoplankton community structure in the western Arctic Ocean: surface layer
589 variability of geographic and temporal considerations in summer. *Hydrobiologia* **811**:
590 295-312.
591 Zabaglo, K., Chrapusta, E., Bober, B., Kaminski, A., Adamski, M., & Bialczyk, J.
592 (2016). Environmental roles and biological activity of domoic acid: A review. *Algal*
593 *Research-Biomass Biofuels and Bioproducts* **13**: 94-101.
594 Zapata, M., Fraga, S., Rodriguez, F., & Garrido, J.L. (2012). Pigment-based chloroplast
595 types in dinoflagellates. *Marine Ecology Progress Series* **465**: 33-+.
596 Zapata, M., Rodriguez, F., Fraga, S., Barra, L., & Ruggiero, M.V. (2011). Chlorophyll c
597 pigment patterns in 18 species (51 strains) of the genus *Pseudo-nitzschia*
598 (Bacillariophyceae). *Journal of Phycology* **47**: 1274-1280.

599

600

601 Table 1. Toxin profiles of three *P. plurisecta* strains including DA and proposed DA
602 isomers according to the available but incomplete standard profile. All toxins are in fg
603 cell^{-1} and "nd" means not detected.

604

***P. plurisecta* strains**	**DA**	**Proposed isomer identities**		
		Iso-DA-D	**Iso-DA-A**	**Epi-DA**
IFR-PPL-15.1	58.3	1.0	3.6	3.1
IFR-PPL-15.2	3.9	nd	0.9	0.5
IFR-PPL-15.3	3.1	nd	0.8	0.5

605

606

607

608

609

610

611 Table 2. Pigment profiles of *P. plurisecta* cells observed in the three strains IFR-PPL-
612 15.1, 15.2 and 15.3 cultivated in batch cultures between 2 to 10 days. Range data (n=10)
613 of average pigment content (n = 3) from triplicate batch cultures over growth are
614 presented as percentage of total pigments (median), cell content in fg $cell^{-1}$ and mol
615 pigment : mol chl *a* and culture content in µg L^{-1}. Pigments are listed in order of
616 decreasing percentage.

Pigments	**% of total pigments**	**Cell content fg $cell^{-1}$**	**Cell content mol: mol chl *a***	**Culture content µg L^{-1}**
Chlorophyll *a*	39 - 50 (48)	157 - 380	-	1.4 - 28.4
Fucoxanthin	29 - 45 (31)	96 - 299	0.834 - 1.439	1.5 - 18.1
Chlorophyll c_3	7 - 10 (8)	23 - 72	0.194 - 0.325	0.3 - 4.0
Chlorophyll c_2	5 - 7 (6)	19 - 54	0.164 - 0.209	0.2 - 3.6
Diadinoxanthin	0 - 7 (4)	0 - 26	0 - 0.218	0 - 3.5
Diatoxanthin	0 - 4 (2)	0 - 17	0 - 0.120	0 - 1.6
β,β-carotene	0 - 2 (0)	0 - 7	0 - 0.058	0 - 0.9

617

618

619

620

621

622

623

624 Figure legends and Figures

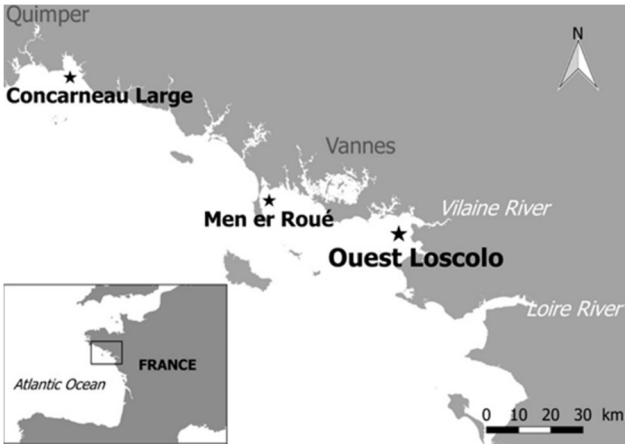

625

626

627 Figure 1. Map of the French Phytoplankton monitoring network sampling sites in the
628 part of the Atlantic Ocean where *P. plurisecta* was observed. At the bottom left-hand
629 corner, the black square shows the site at the scale of the whole France. On the large-
630 scale map, the site "Ouest Loscolo" close to the Vilaine Estuary is indicated by the bold
631 black star. The other sites "Concarneau Large" and "Men er Roué" where *P. plurisecta*
632 was found in 2009 and 2016 respectively, are indicated by small black stars.

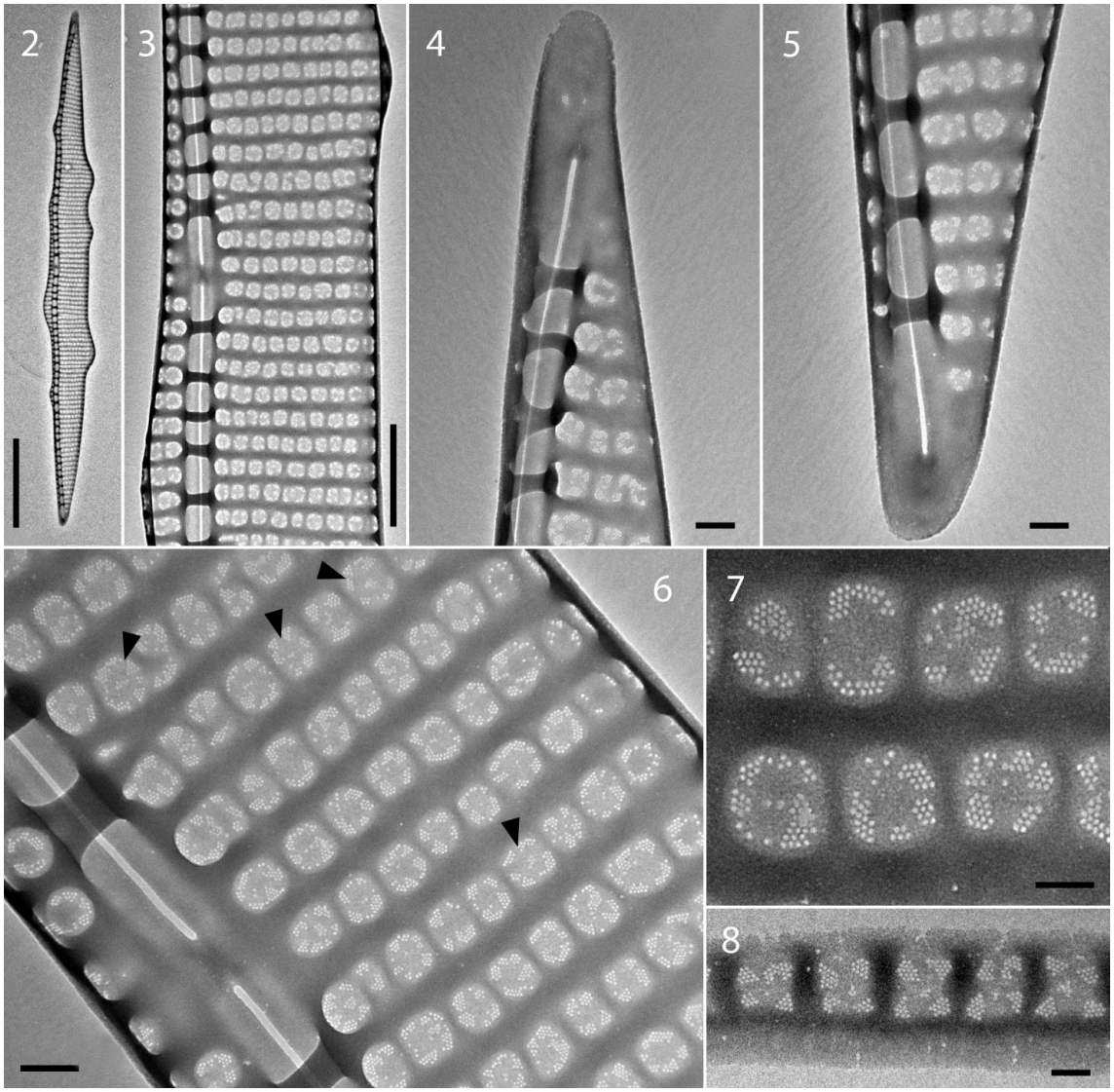

Figures 2-8. TEM photographs of *P. plurisecta* frustules. Fig. 2. Whole valve; Fig. 3. Detail of the central area; Figs 4 & 5. Extremities; Fig. 6. Detail of the central interspace and arrangement of poroids, arrowheads point to poroids with a central sector, in uniseriate striae; Fig. 7. Detail of sectors within poroids; Fig. 8. Detail of poroids in a cingular band. Scale: Fig. 2 = 5 µm; Fig. 3 = 1 µm, Figs. 4 – 6 = 200 nm; Figs. 7 – 8 = 100 nm.

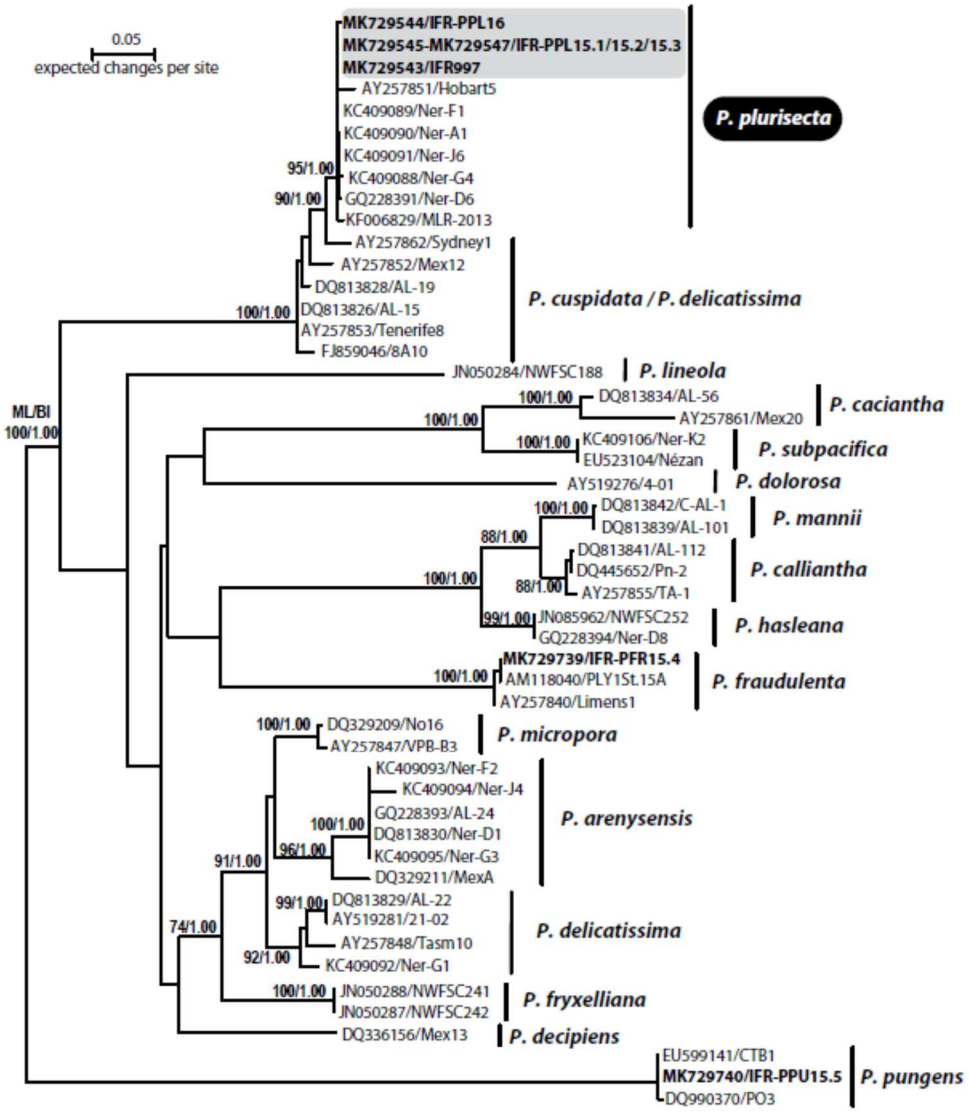

643

644 Figure 9. Maximum likelihood (ML) phylogenetic tree based on ITS rDNA sequences

645 (52 sequences /603 characters). Bootsraps include *x/y* value where *x* is the ML statistic

646 value and *y* is the Bayesian probability.

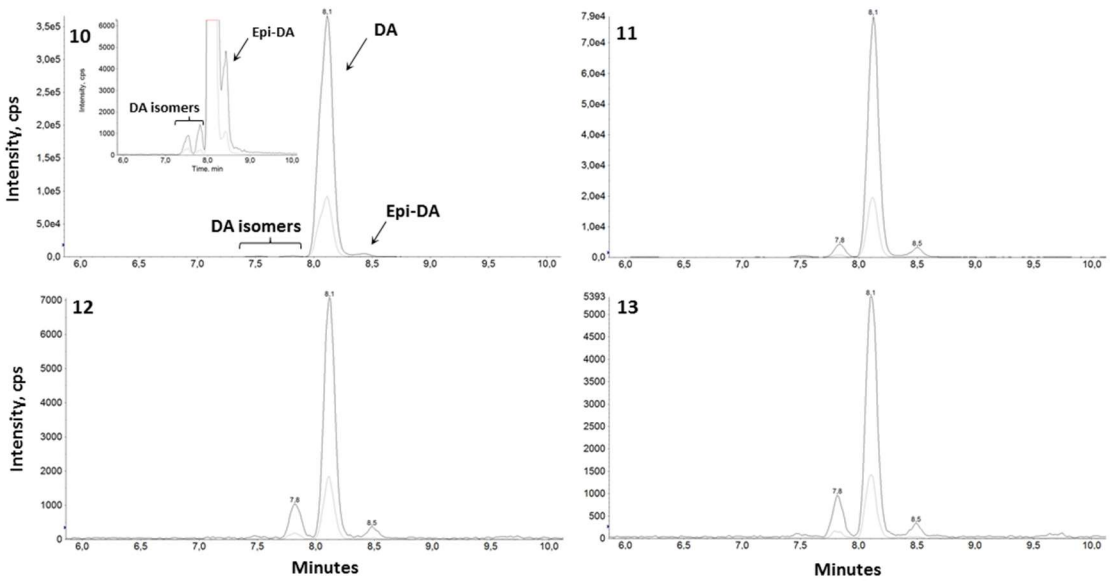

Figures 10-13. Chromatogram of domoic acid (DA) and isomers obtained after LC-MS/MS analyses of standard and *P. plurisecta* cell extracts. Fig. 10. Domoic acid standard; Fig. 11. *P. plurisecta* strain IFR-PPL-15.1; Fig. 12. Strain IFR-PPL-15.2, 13. Strain IFR-PPL-15.3. Figures 10 and 11 include magnified views to show the isomer peaks. The highest peak represents the most abundant *m/z* transition 312.1 → 266.1 and the peak beneath is the less intense fragment 312.1→ 161.1.

Figure S1 Photographs of *Pseudo-nitzschia fraudulenta* IFR-PFR-15.4 acquired by scanning electron microscopy

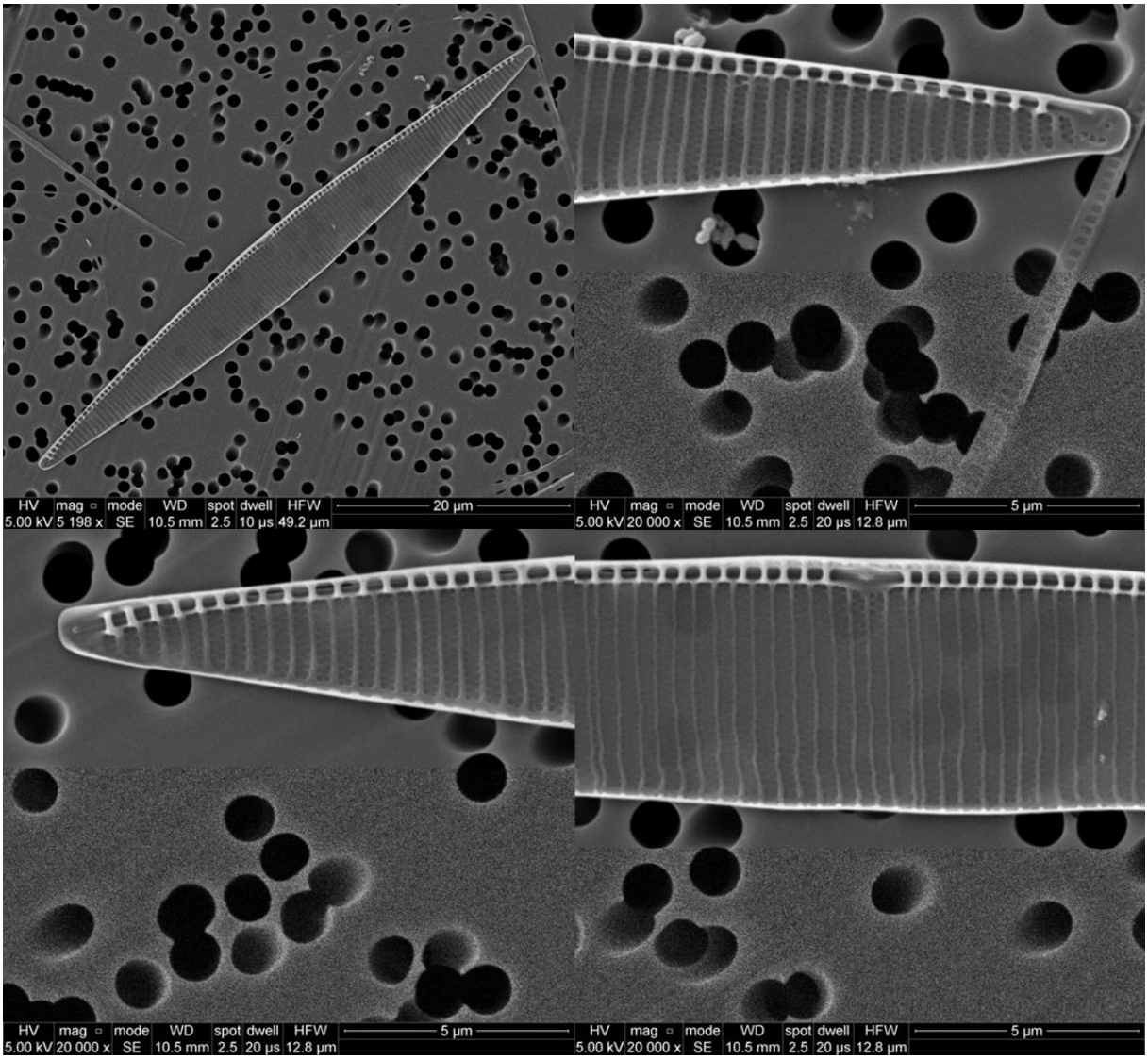

Figure S2 Photographs of *Pseudo-nitzschia pungens* IFR-PPU-15.5 acquired by scanning electron microscopy